Journal of Alloys and Compounds 509 (2011) 5095–5098

Contents lists available at ScienceDirect

Journal of Alloys and Compounds

journal homepage: www.elsevier.com/locate/jallcom

Synthesis of cadmium oxide doped ZnO nanostructures using electrochemical deposition

Trilok Singh*, D.K. Pandya, R. Singh

Department of Physics, Indian Institute of Technology Delhi, Hauz Khas, New Delhi 110016, India

ARTICLE INFO

Article history:
Received 4 September 2010
Accepted 30 January 2011
Available online 1 March 2011

Keywords:
ZnCdO
Electrodeposition
Nanostructures
Bandgap

ABSTRACT

Ternary ZnCdO alloy semiconductor nanostructures were grown using electrochemical deposition. Crystalline nanostructures/nanorods with cadmium concentration ranging from 4 to 16 at% in the initial solution were electrodeposited on tin doped indium oxide (ITO) conducting glass substrates at a constant cathodic potential −0.9 V and subsequently annealed in air at 300 °C. X-ray diffraction measurements showed that the nanostructures were of wurtzite structure and possessed a compressive stress along the *c*-axis direction. The elemental composition of nanostructures was confirmed by energy dispersive spectroscopy (EDS). ZnO nanostructures were found to be highly transparent and had an average transmittance of 85% in the visible range of the spectrum. After the incorporation of Cd content into ZnO the average transmittance decreased and the bandgap tuning was also achieved.

1. Introduction

Nanostructured materials have attracted great interest due to their unique chemical and physical properties, which can be influenced not only by the preparation procedure but also by their shape and size [1–7]. The morphology of the nanostructures plays a key role especially on the optoelectronic properties of the materials, which determine the performance of semiconductors to be used in solar cells [9], ultraviolet lasers [8], sensors [10,11], photo transistors and diodes [12]. Among group II–VI semiconductor materials, ZnO is one of the most attractive functional semiconductor material for the fabrication of optoelectronic devices operating in the blue and ultraviolet region because of a direct wide band-gap of 3.37 eV and an exciton binding energy of 60 meV [13,14]. It is well known that the realization of bandgap engineering to create barrier layers and quantum wells in device heterostructure is an important step for the design of ZnO-based devices. CdO is an *n*-type semiconductor with a direct band-gap of 2.3 eV and an indirect band-gap of 1.36 eV [15]. The ternary $Zn_{1-x}Cd_xO$ alloy can allow the bandgap tuning from 3.37 eV (band-gap of ZnO at room temperature) to a narrower bandgap [16]. The control over morphology and size of semiconductor materials represents a great challenge in realizing the design of novel functional devices. Li et al. studied the growth and optical properties of ZnCdO nanorods grown on copper substrate [20]. Recently, Pillai et al. have investigated effect of Cd incorporation on the microstructural and optical properties [18]. Mahmoud et al. have studied the influence of temperature on the structures of Cd-doped ZnO nanopowders [19]. In this article, we have carried out an electrodeposition of ZnCdO nanostructures in ITO substrate to study the effect of low Cd concentration in structural and optical properties of ZnO. The electrochemical deposition allows mixing of the chemicals at atomic level thus reducing the possibility of undetectable impurity phases [20] and it is a good candidate to solve the problem of the small thermodynamic solubility of CdO in ZnO [21]. Furthermore, the electrochemical deposition presents a simple, quick and economical method for the preparation of $Zn_{1-x}Cd_xO$ nanostructures.

2. Experimental

The electrodeposition process was carried out in a specially designed closed glass cell. The indium doped tin oxide (ITO) transparent glass substrate was used as a working electrode while platinum sheet and saturated calomel electrode (SCE) were used for counter and reference electrodes, respectively. The electrolyte (bath) temperature was varied from 80 to 90 °C. The ITO glass substrate was cleaned ultrasonically in acetone, toluene and then rinsed in deionized water for three times. For the growth of ternary compound nanostructures the precursor solutions were obtained by varying the zinc nitrate and cadmium nitrate concentrations in deionized water. The cadmium concentration for the growth of nanostructures was varied from 4 to 16 at% in the initial solution. The electrochemical depositions of ternary ZnCdO compounds were carried out at the deposition potential of −0.9 V (vs. SCE) for 20 min. After the deposition the sample was removed from electrolyte and rinsed in de-ionized water. For the structural studies, X-ray diffractometer (Philips Xpert Pro) using CuK_α ($\lambda = 1.5405$ Å) radiation in 2θ range 20–80° was used. Scanning electron microscopy images were obtained using EVO-50 model from ZEISS. Energy dispersive X-ray spectroscopy was obtained from Bruker-ASX (Model Quan-Tax 200). The transmission spectra of grown nanostructures were measured using UV-VIS spectrometer from Perkin Elmer (Model Lambda 650).

* Corresponding author at: Department of Physics, Thin Film Laboratory, Indian Institute of Technology Delhi, Hauz Khas, New Delhi 110016, India.
Tel.: +91 011 2659 6658; fax: +91 011 2658 1114.
E-mail address: trilok_ph@student.iitd.ac.in (T. Singh).

0925-8388/$ – see front matter © 2011 Elsevier B.V. All rights reserved.
doi:10.1016/j.jallcom.2011.01.168

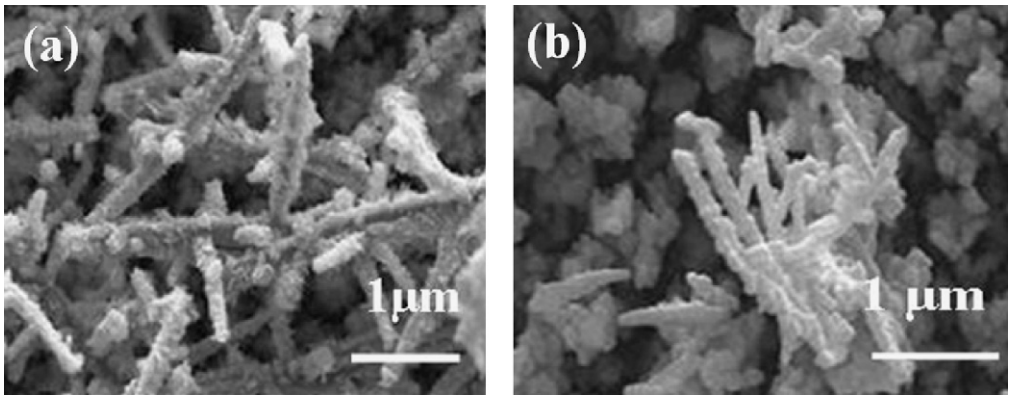

Fig. 1. SEM Images of ZnCdO nanorods with (a) 9 at% and (b) 16 at% Cd grown at 85 °C, annealed at 300 °C in air ambient.

3. Results and discussion

Fig. 1a and b shows the SEM image of the prepared sample on the ITO substrate. The products are observed as nanostructures with diameters of 150–200 nm on the substrate. The length of nanostructures is up to a few micrometers. It is interesting that there is no smoothness on the sidewall, which is different from quasi aligned nanorods with smooth surface synthesized via physical vapor deposition method [22]. In general, it is well-known that the surface/volume ratio in the nanostructure can greatly influence properties of nanomaterials and application in the nanodevice. At present, the successful synthesis of ternary compound (ZnCdO) nanostructures with high surface/volume ratio enriches the family of CdO, ZnO and ZnCdO nanomaterials, which can prompt their applications. The chemical composition of ZnCdO nanostructures was obtained from EDS. Fig. 2 shows a typical EDS spectrum for a ZnCdO sample. Different elements contents are observed in the spectrum and it confirms the presence of Cd and Zn. The aqueous solution of $Zn(NO_3)_2$ and $Cd(NO_3)_2$ were taken as a source of precursors for Zn and Cd respectively. The electrolyte dissociate in the aqueous solution and nitrate ions (NO_3^-) is electro-reduced to hydroxide ions (OH^-) via Eq. (1) [23]. The produced OH^- react with Zn^{2+} to form $Zn(OH)_2$ and this leads to the formation of ZnO via Eq. (2). On the other hand Cd^{2+} ions react with hydroxyl ions to form CdO via Eq. (3). Finally, ZnO and CdO mix at atomic levels and formed ZnCdO alloy [17].

$$NO_3^- + H_2O + 2e^- \rightarrow NO_2^- + 2OH^- \quad (1)$$

$$2OH^- + Zn^{2+} \rightarrow Zn(OH)_2 \rightarrow ZnO + H_2O \quad (2)$$

$$Cd^{2+} + 2OH^- \rightarrow Cd(OH)_2 \rightarrow CdO + H_2O \quad (3)$$

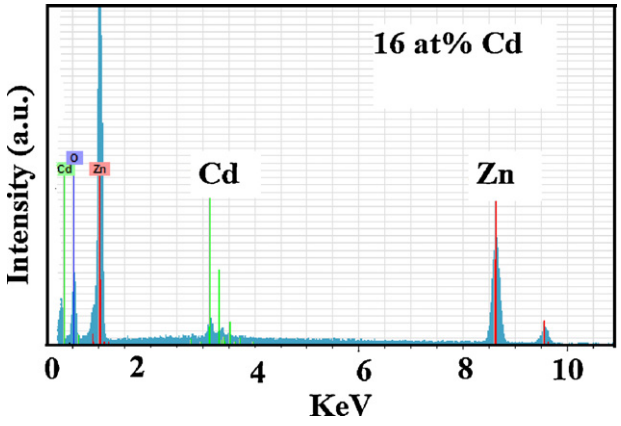

Fig. 2. EDS spectrum of 16 at% Cd doped ZnO nanorods.

$$(1-x)ZnO + xCdO \rightarrow Zn_{1-x}Cd_xO \quad (4)$$

The XRD patterns of electrodeposited ternary compound for grown samples with different Cd concentrations are shown in Fig. 3. The diffraction peaks were identified as belonging to wurtzite phase of ZnO. The XRD patterns of ternary compounds are similar to the electrodeposited ZnO nanostructures with dominant reflection planes (1 0 0), (0 0 2), (1 0 1), (1 0 2), (1 1 0) and (1 0 3). Dominant reflection planes reveal that the synthesized ternary compound are of the hexagonal wurtzite ZnO structure without any impurity phases, especially Zn, Cd and CdO. Notably, the XRD patterns exhibits (0 0 2)-preferred orientation. The (0 0 2) (inset in Fig. 3) peak for 16 at% Cd is at 34.28°, slightly shifted towards the low-angle side when compared with that of pure ZnO (34.42°), implying the existence of compressive stress in the *c*-axis orientation. The lattice expansion indicates that the substitution of the smaller Zn atom (with an ionic radius 0.06 nm) by the larger Cd atom (with an ionic radius 0.074 nm) takes place on the equivalent crystallographic position of Zn in the hexagonal wurtzite structure. Moreover, no peaks corresponding to CdO are observed up to 16 at% Cd content. Hence the peaks observed in Fig. 3 are related to the wurtzite structure. For the bulk ZnO the reported values of the lattice constants are $a = b = 3.249$ Å and $c = 5.205$ Å [JCPDS Card No. 79-0206]. It was observed that the incorporation of Cd into ZnO changed the full width at half maxima (FWHM) of (0 0 2) peak in XRD (Fig. 4a) and the lattice constants *a*- and *c*-were also vary as a function of Cd concentration values (Fig. 4b) [24]. The lattice

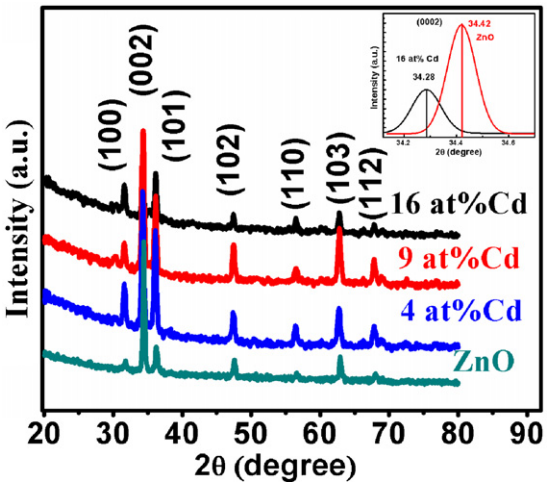

Fig. 3. XRD patterns of cadmium doped ZnO nanorods with 4 at% Cd, 9 at% Cd and 16 at% Cd. The inset shows the magnified spectrum of (0 0 2) peak of ZnO and 16 at% Cd nanostructures.

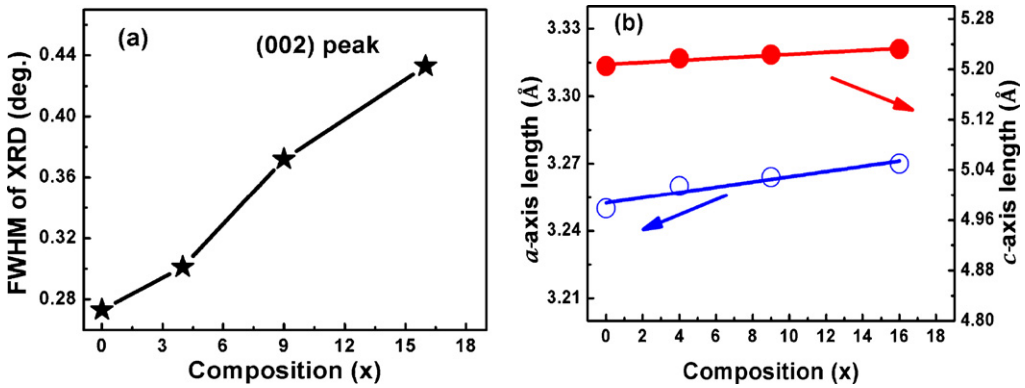

Fig. 4. Cadmium content dependence of (a) FWHM values of the (0 0 2) peak in the XRD θ–2θ scanned curves, and (b) dependence of the a- and c-axis lattice lengths of the $Zn_{1-x}Cd_xO$ nanostructures grown on ITO substrates.

Table 1
Structural and optical constants of electrodeposited nanostructures undoped and CdO doped ZnO samples annealed at 300 °C.

Sample	Lattice parameters (Å) $a=b$	Lattice parameters (Å) c	Bi-axial stress (GPa)	Bandgap energy E_g (eV)	T (%)
ZnO	3.25	5.205	0	3.32	85
4 at% Cd	3.260	5.217	-0.448×10^9	3.25	70
9 at% Cd	3.264	5.223	-1.030×10^9	3.17	65
16 at% Cd	3.270	5.232	-1.433×10^9	3.08	58

constants a, b and c of nanostructures are calculated and given in Table 1. The samples with c-values greater than the bulk value have a positive or extensive strain whereas those with lower values have a negative or compressive strain. Thus the undoped ZnO has no strain while Cd doped ZnO has very less compressive strain. The lattice stress σ_f of the nanostructures has been calculated (Table 1) using the expression [18].

$$\sigma_f = 2.33 \times 10^{11} \times \frac{c_b - c_f}{c_b} \quad (5)$$

where c_b and c_f are the lattice constant c of the bulk ZnO and grown nanostructure films, respectively. The negative sign of estimated stress for the doped ZnO indicates that the crystallites are under a state of compressive stress. The transmittance spectra of the grown nanostructures were measured to investigate the optical properties of the ternary compound. The ZnO is highly transparent and has an average transmittance of 85% in the visible region. When the concentration of Cd increases in the starting solution, one can observe change in the cut-off wavelength and the decrease in average transmittance in the near visible and visible region. This is due to the incorporation of Cd contents in the deposit and the replacement of Zn atoms by Cd atoms which is also confirmed from XRD measurement. When more Cd contents were incorporated into ZnO, the bandgap of ternary $Zn_{1-x}Cd_xO$ will become narrower. This will lead to more oxygen vacancies and cadmium/zinc interstitials. This leads to higher carrier concentration and consequently, will reduce the optical transmittance [17,25]. Hence, the optical transmittance for the sample with 16 at% Cd is reduced from 85 to 58%. The direct allowed optical band gap E_g could be determined with the help of standard relation [26].

$$\alpha h\nu = A(h\nu - E_g)^m \quad (6)$$

where A is an energy-independent constant, E_g is the optical band gap and m is the constant which determine type of optical transition. The optical band gap tuning of ZnCdO alloys was achieved up to 0.24 eV (Fig. 5) and the bandgap become narrower with the higher Cd incorporation in the ZnO nanostructures (in the inset of Fig. 5). These results depict the bandgap engineering of ternary compound $Zn_{1-x}Cd_xO$.

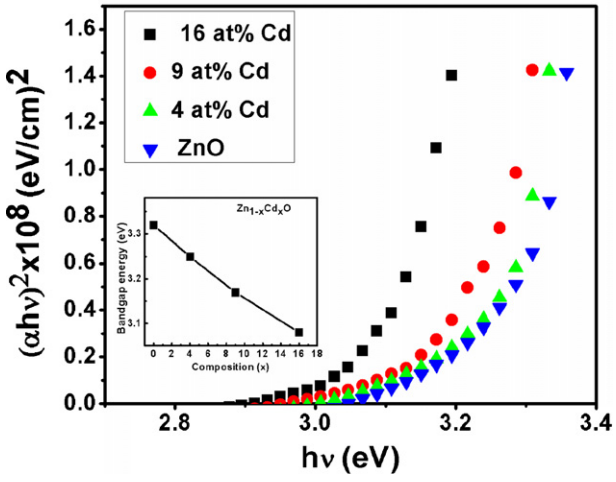

Fig. 5. $(\alpha h\nu)^2$ vs. photon energy of ZnO and ZnCdO nanostructures. The inset shows the bandgap variation with Cd concentration.

4. Conclusions

We have shown that the electrodeposition is an effective technique to obtain ternary $Zn_{1-x}Cd_xO$ nanostructures such as nanorods, with high aspect ratio (~20–25). The nanostructures were synthesized on ITO by electrodeposition at low temperature (<90 °C), and subsequently annealed at 300 °C in air ambient for 1 h. No morphological changes were observed in all samples at this annealing temperature. XRD analysis showed the $Zn_{1-x}Cd_xO$ nanostructures possessed pure ZnO wurtzite structure. It was also observed that for low Cd concentration in the primary solution there was compressive stress in the c-axis direction and the compressive stress varied from 0 to 1.44×10^9 GPa for x = 0–16 at% ($Zn_{1-x}Cd_xO$). The cut-off wavelength shifted from blue to red on account of the Cd incorporation in the ZnO and the average transmittance decreased by ~31%. The bandgap tuning for 4–16 at% Cd in the initial solution was achieved in the range of 3.32–3.08 eV (up to 0.24 eV).

Acknowledgements

The authors gratefully thank the XRD and SEM measurement facilities of IIT Delhi. One of the authors (Trilok Singh) acknowledges IIT Delhi for providing research fellowship.

References

[1] A.P. Alivisatos, Science 271 (1996) 933–937.
[2] C.M. Lieber, Solid State Commun. 107 (1998) 607–616.
[3] H. Tang, H. He, L. Zhu, Z. Ye, M. Zhi, F. Yang, B. Zhao, J. Phys. D: Appl. Phys. 39 (2006) 3764–3768.
[4] M. Tortosa, M. Mollar, B. Mari, J. Cryst. Growth 304 (2007) 97–102.
[5] G. Wang, Z. Ye, H. He, H. Tang, J. Li, J. Phys. D: Appl. Phys. 40 (2007) 5287–5290.
[6] S. Vijaylakshmi, S. Venkataraj, R. Jayavel, J. Phys. D: Appl. Phys. 41 (2008) 245403–245409.
[7] Y. Caglar, M. Caglar, S. Iliha, A. Ates, J. Phys. D: Appl. Phys. 42 (2009) 065421–065428.
[8] M. Lorie, J.G. Johnson, R. Saykally, D.P. Yang, Nat. Mater. 4 (2005) 455–459.
[9] H.M. Huang, S. Mao, H. Feick, Q.H. Yan, Y.Y. Wu, H. Kind, E. Weber, R. Russo, D.P. Yang, Science 292 (2001) 1897–1899.
[10] H.J. Lim, K.C. Kang, K.K. Kim, K.I. Park, K.D. Hwang, J.S. Park, Adv. Mater. 18 (2006) 2720–2724.
[11] W.C. Cheng, Y.G. Xu, Q.H. Zhang, Y. Luo, J. Nanosci. Nanotechnol. 7 (2007) 4345–4439.
[12] W.C. Cheng, Y.G. Xu, Q.H. Zhang, Y. Luo, G.P. Zhang, K. Shen, Mater. Res. Bull. 43 (2008) 3506–3513.
[13] V.E. Henrich, P.A. Cox, The Surface Science of Metal Oxides, Cambridge University Press, Cambridge, 1994.
[14] H. Cao, J.Y. Xu, D.Z. Zhang, S.H. Chang, S.T. Ho, E.W. Seelig, X. Liu, R.P.H. Chang, Phys. Rev. Lett. 84 (2000) 5584–5587.
[15] I.D. Makuta, S.K. Poznyak, A.I. Kulak, E.A. Streltsov, Phys. Status Solidi A 111 (1989) 193–199.
[16] C.X. Shan, Z. Liu, Z.Z. Zhang, D.Z. Shen, S.K. Hark, J. Phys. Chem. B 110 (2006) 11176–11179.
[17] L.G. Ren, Z.W. Xia, B. Qiong, T.Y. Xiang, Electrochem. Commun. 11 (2009) 282–285.
[18] R.V. Kumar, K.J. Lethy, P.R. Arunkumar, R.R. Krishnan, N.V. Pillai, V.P.M. Pillai, R. Philip, Mater. Chem. Phys. 121 (2010) 406–413.
[19] W.E. Mahmoud, A.A. Al-Ghamdi, S. Al-Heniti, S. Al-Ameer, J. Alloys Compd. 491 (2010) 742–746.
[20] Y.J. Li, C.Y. Wang, M.Y. Lu, K.M. Li, L.J. Chen, Cryst. Growth Des. 8 (2008) 2598–2602.
[21] F. Bertram, S. Giemsch, D. Forster, J. Christen, R. Kling, C. Kirchner, A. Waag, Appl. Phys. Lett. 88 (2006) 061915–061917.
[22] F. Wang, H. He, Z. Ye, L. Zhu, H. Tang, Y. Zhang, J. Phys. D: Appl. Phys. 38 (2005) 2919–2922.
[23] L. Xu, Q. Chen, D. Xu, J. Phys. Chem. C 111 (2007) 11560–11565.
[24] T. Makino, Y. Segawa, M. Kawasaki, A. Ohtomo, R. Shiroki, K. Tamura, T. Yasuda, H. Koinuma, Appl. Phys. Lett. 78 (2001) 1237–1239.
[25] T.K. Subramanyam, B.S. Naidu, S. Uthana, Appl. Surf. Sci. 529 (2001) 169–170.
[26] J. Hu, R.G. Gordon, J. Appl. Phys. 71 (1992) 880–890.